Influence of Tip Clearance on Forced Convection Heat Transfer of a Finned Plate in a Duct

Hae-Kyun Park and Bum-Jin Chung*
Department of Nuclear Engineering, Kyung Hee University
#1732 Deokyoung-daero, Giheung-gu, Yongin-si, Gyeonggi-do, 446-701, Korea
Corresponding author: bjchung@khu.ac.kr

1. Introduction

Finned plates have been used widely to enhance the cooling capability of a system. There are numerous studies for forced convection condition. Fins increase the heat transfer areas and enhance the heat transfers. Meanwhile, they also increase the pressure drops and impair the heat transfer. Thus optimizations are required for a proper enhancement of cooling capability [1].

An important phenomenological consideration is to be reveals for a finned plate in a duct. Due to the high friction near the fin region and low friction near the wall region, the forced flow tends to bypass from fin region to wall region. The bypass flow increases the net flow and enhances the heat transfer for a moderate tip clearance which is defined by the distance from the tip of the fin and the wall [2]. Meanwhile for a large tip clearance, most of the flow bypasses and does not contribute the heat transfer and impairs the heat transfer [3].

This study is a preliminary numerical study on the influence of the tip clearance on the heat transfer of the finned plate in a duct. The study aimed at supporting an experimental research exploring the phenomena for a very small tip clearance. Thus material properties and test conditions were chosen to meet the experimental conditions. It investigated the phenomena at Pr of 2,014 and ReS of 58.3.

2. Methods of Analysis

2.1 Test model

The test model geometry and material properties are indicated on Tables I and II respectively.

Table I: The test model geometry.

Fin height (H)	0.005m
Fin spacing (S)	0.002m
Plate Length (L)	0.05m
Tip clearance	0.005m

Table II: The test model material properties.

Density	1096.6 kg/m^3
Specific heat	1000 J/kg-K
Thermal conductivity	6.23×10^{-4} W/m-K
Viscosity	1.253×10^{-3} kg/m-s
Pr	2,014
Re_S	58.3

Governing equations and boundary conditions are listed in Equations (1)-(6).

$$\frac{\partial u_i}{\partial x}+\frac{\partial u_j}{\partial y}+\frac{\partial u_k}{\partial z}=0. \quad (1)$$

$$u_i\frac{\partial u_i}{\partial x}+u_j\frac{\partial u_i}{\partial y}+u_k\frac{\partial u_i}{\partial z}=\nu\left(\frac{\partial^2 u_i}{\partial x^2}+\frac{\partial^2 u_i}{\partial y^2}+\frac{\partial^2 u_i}{\partial z^2}\right)-\frac{1}{\rho}\frac{\partial p}{\partial x}, \quad (2a)$$

$$u_i\frac{\partial u_j}{\partial x}+u_j\frac{\partial u_j}{\partial y}+u_k\frac{\partial u_j}{\partial z}=\nu\left(\frac{\partial^2 u_j}{\partial x^2}+\frac{\partial^2 u_j}{\partial y^2}+\frac{\partial^2 u_j}{\partial z^2}\right)-\frac{1}{\rho}\frac{\partial p}{\partial y}, \quad (2b)$$

$$u_i\frac{\partial u_k}{\partial x}+u_j\frac{\partial u_k}{\partial y}+u_k\frac{\partial u_k}{\partial z}=\nu\left(\frac{\partial^2 u_k}{\partial x^2}+\frac{\partial^2 u_k}{\partial y^2}+\frac{\partial^2 u_k}{\partial z^2}\right)-\frac{1}{\rho}\frac{\partial p}{\partial z}. \quad (2c)$$

$$u_i\frac{\partial T}{\partial x}+u_j\frac{\partial T}{\partial y}+u_k\frac{\partial T}{\partial z}=\alpha\left(\frac{\partial^2 T}{\partial x^2}+\frac{\partial^2 T}{\partial y^2}+\frac{\partial^2 T}{\partial z^2}\right). \quad (3)$$

$u_i=u_k=0$ and $u_j=u_{in}$ at inlet. (4)

$u_i=u_j=u_k=0$ and $T=T_0$ on heated wall. (5)

$u_i=u_j=u_k=0$ and $T=T_\infty$ as fluid. (6)

2.2 Numerical analysis

The numerical analysis was performed using FLUENT ver. 6.3.26) [4]. Figs. 1 and 2 shows the simulated geometry. The optimized cell number of about 2.4×10^5 cells, was obtained by performing a sensitivity analysis.

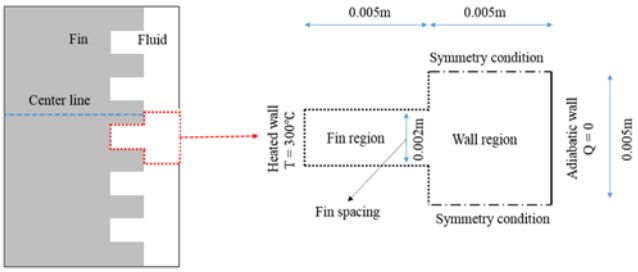

Fig. 1. Plane view of the simulated geometry.

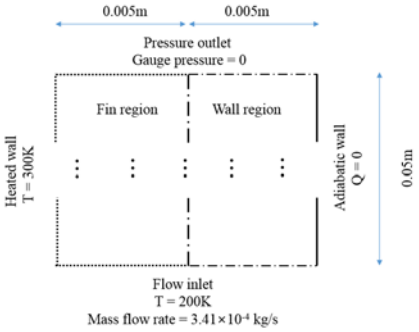

Fig. 2. Side view of the simulated geometry.

A second-order upwind scheme for energy and momentum equations and the SIMPLE algorism were used.

3. Results and Discussion

The error of the calculated Nu_S was 12% when compared with the experimental result performed for the same material properties and temperature conditions.

3.1 Velocity profiles

The cross sectional velocity profiles are shown in the Figs. 3 and 4.

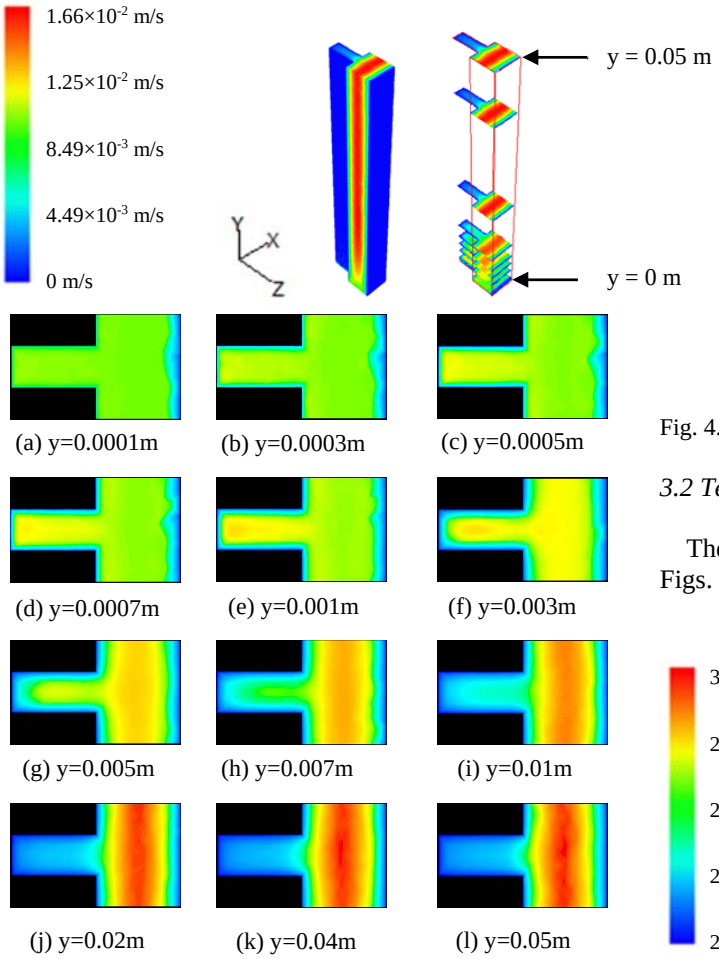

Fig. 3. Velocity fields at each elevation.

As shown in Fig. 3 (a)-(d), the velocity boundary layers develop along the flow direction at both fin and wall regions. Fig. 3 (e)-(i) show the reduced flow velocities in the fin region and enhanced flow velocities in the wall region, which means the flows bypass to wall region due to the higher friction in the fin region. Fig. 3 (j) shows that the boundary layers developed from each fin surfaces meet and the flow in the fin region becomes fully developed.

Figure 4 presents the cross sectional velocity profiles along the duct, which shows the bypass flow increases along the duct. At an elevation between 0.01m and 0.02m, the velocity profiles become fully developed.

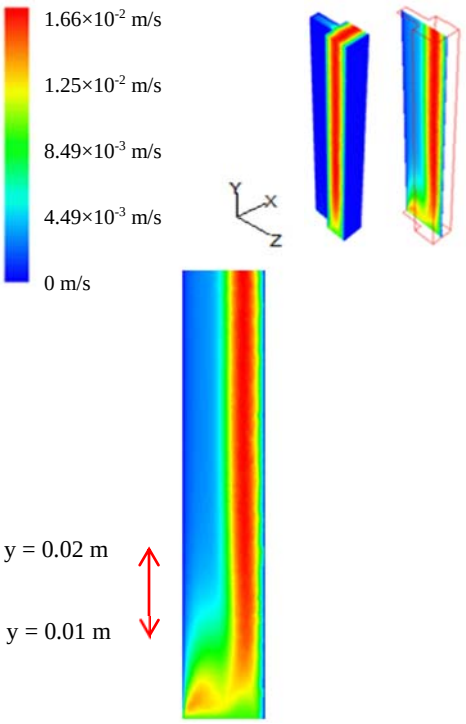

Fig. 4. Cross sectional velocity fields along the duct.

3.2 Temperature profiles

The cross sectional temperature profiles are shown in Figs. 5 and 6.

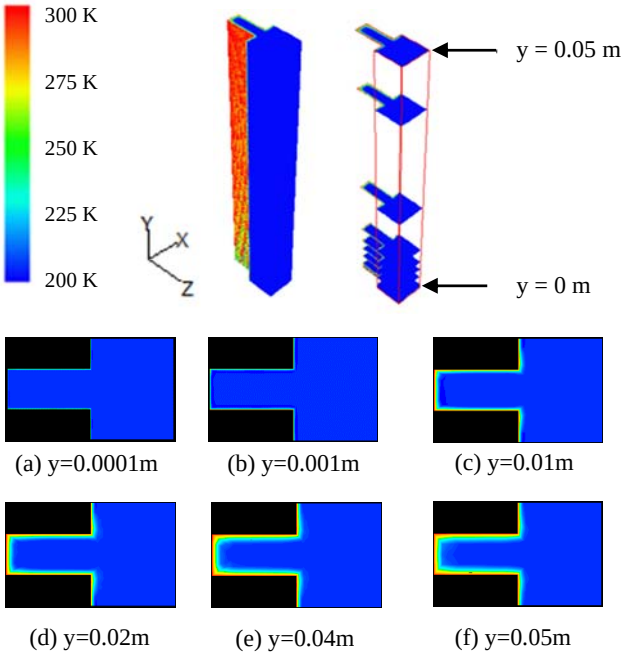

Fig. 5. Temperature fields at each elevation.

Fig. 5 shows the cross sectional temperature fields at each elevation of the duct. The thermal boundary layers are significantly slender compared to the momentum boundary layers. This is due to the large Prandtl number value of the working fluid. The thermal boundary layers develop along the duct. Thicker boundary layers are observed at the corner connecting the base plate and the fin, which impair the heat transfers.

Fig. 6 presents the cross sectional temperature fields along the duct. Fig. 6 (a) shows the temperature profile at the heated wall, which is fixed to constant temperature of 300K. Fig. 6 (b)-(g) show the temperature decreases with z. The bottom parts of the figures show the cooling by the flows. The temperature profiles of Fig. 6 (g)-(k) seem to be unchanged due to the fully developed flow conditions.

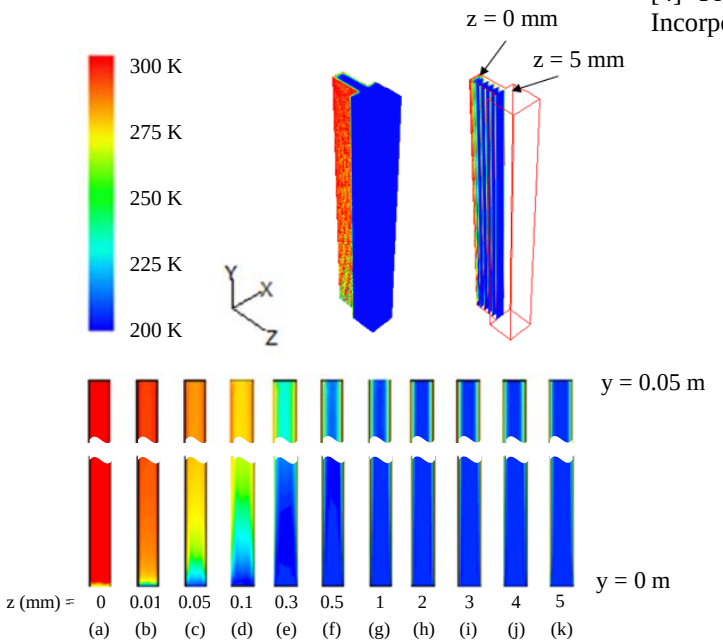

Fig. 6. Cross sectional temperature fields along the duct.

4. Conclusions

In order to investigate the small tip clearance phenomena, a simple numerical scheme was developed using a commercial CFD code. A case with the same experimental condition was tested using the numerical scheme and the error was about 12%.

The results show the clear evidence of the flow bypass from the fin region to wall region, which impair the heat removal capacity of the finned plate in a duct.

The study has the relevance with the reactor cavity cooling system performance enhancement activities in the VHTR. The numerical scheme will be tested for narrower and wider tip clearances and find an optimal tip clearance.

REFERENCES

[1] H. Shaukatullah, Wayne R. Storr, Bernt J. Hansen, Michael A. Gaynes, Design and optimization of pin fin heat sinks for low velocity application, 12th IEEE Semi-Therm Symposium, pp. 151-163, 1996.

[2] Jin Wook Kim, Sang Hoon Kim, “Effect of a flow barrier on the cooling performance for a straight fin heat sink with bypass flow,” Transactions of the KSME, pp. 93-98, 2009.

[3] Saad A. El-Sayed, Shamloul M. Mohamed, Ahmed M. Abdel-latif, Abdel-hamid E. Abouda, Investigation of turbulent heat transfer and fluid flow in longitudinal rectangular-fin arrays of different geometries and shrouded fin array, Experimental Thermal and Fluid Science, Vol. 26, pp. 879-900, 2002.

[4] Fluent User’s Guide (2006) release 6.3 Fluent Incorporated.